# 薄板钛合金激光焊熔透稳定性临界条件的计算

陈 俐[1,2], 胡伦骥[1], 巩水利[2]
(1 华中科技大学 材料科学与工程学院, 武汉 430074; 2 北京航空制造工程研究所 高能束流加工技术国防科技重点实验室, 北京 100024)

摘 要: 钛合金薄板熔透激光焊研究发现, 在一定焊接参数条件下, 由于金属蒸气和光致等离子体的作用, 即使焊接过程的工艺参数稳定不变, 也存在全熔透不稳定过程, 其特征是焊缝表面成形均匀不变, 而焊缝背面出现熔透与未熔透之间交替跳跃的成形特征, 这种不稳定焊接过程属于激光深熔焊过程的本征特性, 主要取决于焊接过程穿孔形成的稳定性。基于小孔形成机理和孔壁能量平衡的分析, 提出了小孔穿孔速度与焊接速度相匹配的熔透稳定性物理模型, 将穿孔速度与激光功率密度、焊接速度、材料物理性能、板厚联系起来, 并建立了熔透焊所需最小激光功率密度计算关系式, 理论计算结果与试验结果基本一致。所建立的关系式可用于判断焊接工艺参数深熔焊熔透稳定性。

关键词: 钛合金; 激光焊; 全熔透焊接; 焊接稳定性计算
中图分类号: TG46 7 文献标识码: A 文章编号: 0253-360X(2005)11-35-04

陈 俐

## 0 序 言

具有小孔效应的激光深熔焊是激光焊接应用的主要模式, 但伴随小孔形成而产生的金属蒸气和光致等离子体影响金属对激光能量的吸收, 易导致不稳定焊接过程。已有研究发现, 激光焊在一定焊接条件下会产生稳定热导焊模式和稳定深熔焊模式间来回跳变的不稳定焊接过程, 焊缝熔深和熔宽无规则地剧烈波动[1~3]。该过程不是由于焊接工艺参数不稳定而引起的偶然现象, 而是激光焊所固有的特性。当激光功率密度在小孔产生阈值的附近, 因等离子体 金属蒸气云对激光的吸收、散射和折射作用, 使作用到金属表面的激光功率密度产生波动, 即导致了这种不稳定过程。对于激光焊出现的模式跳变不稳定, 有学者提出了稳定激光焊接过程的工艺参数双 U形控制曲线。通过确定稳定热导焊的上临界激光功率密度和稳定深熔焊的下临界功率密度, 可避免激光焊模式跳变不稳定过程的产生。

此外, 在实际应用中, 薄板焊接一般要求熔透焊, 这使得保证激光焊过程全熔透稳定性往往是必须的, 尤其是长焊缝的焊接, 但有关薄板大功率激光熔透焊缝成形不稳定性的研究却少有涉及。作者针对 2.5mm厚钛合金研究了激光深熔焊的焊缝熔透成形不稳定性, 以及全熔透焊的稳定条件, 以便为实际应用中激光焊工艺参数的确定提供理论基础。

收稿日期: 2005-09-21
基金项目: 国家教委博士点基金资助项目(20030487029); 航空基金资助项目(01H25007)

## 1 薄板激光全熔透焊的不稳定性

### 1.1 试验条件与试验方法

研究材料为近 α相钛合金, 名义成分 Ti-6.5Al-2Zr-1Mo-1V。试板尺寸 250 mm × 100 mm × 2.5mm, 焊前酸洗处理, 焊接过程在专用夹具上完成, 利用激光焊接头同轴保护气、托罩保护气和焊接夹具上紫铜槽背面保护气对焊接熔池、焊缝上下表面保护, 气流量分别为 6 L/min、15 L/min、10 L/min, 保护气采用氩气。焊接设备为 PRC4000快速轴流 $CO_2$ 激光器和 AM 356YAG激光器, 透镜焦长分别 190mm和 200mm, 焦斑直径分别为 0.38mm和 0.6mm。线切割切取纵向和横向焊缝截面试样, 观察焊缝成形。

### 1.2 试验结果与分析

无论是 $CO_2$ 激光焊, 还是 YAG激光焊, 焊接工艺参数不同得到的焊接成形特征不同。图 1是离焦量为 -0.5mm时激光功率和焊接速度变化的全熔透焊缝成形, 有钉头形和沙漏形两种特征, 这种焊缝成形特征变化与焊接热输入和激光功率密度相关。在所研究条件下, 缝宽比 (焊缝背面熔宽与正面熔宽之比)小于 0.4时, 即使焊接过程工艺参数稳定

不变, 全熔透焊缝成形易出现焊缝表面成形良好, 而焊缝背面出现熔透与未熔透间的跳变, 见图 2.

和焊接模式在热导焊与深熔焊间跳变的不稳定焊过程相比, 全熔透焊不稳定形成的焊缝成形特征是不一样的。研究表明, 对一定的板厚, 激光功率和激光功率密度足够, 激光深熔焊可形成穿透性小孔, 否则形成盲孔。若激光功率密度处于穿孔的阈值附近, 焊接过程在熔透和未熔透之间波动, 导致全熔透焊过程不稳定。其原因是由于光致等离子体 金属蒸气云的影响, 削弱了激光对钛合金的作用。显然, 熔透不稳定与焊接过程穿孔稳定性密切相关, 而且同稳定热导焊和稳定深熔焊一样, 稳定激光熔透深熔焊也存在一个激光功率密度阈值。

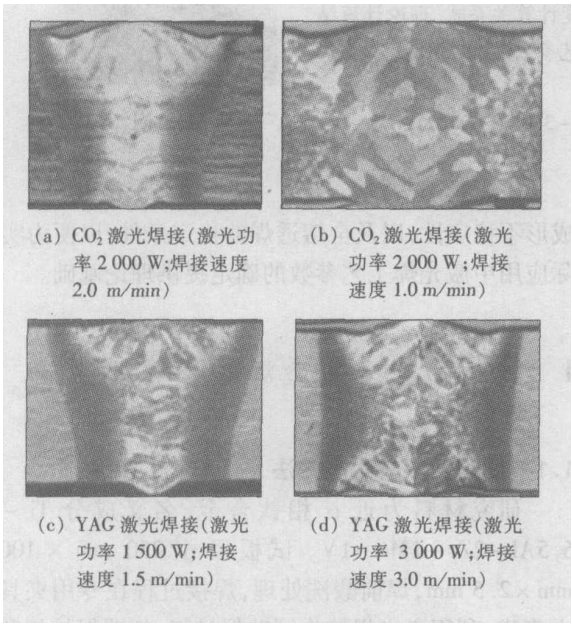


图 1 BT20钛合金激光焊焊缝横截面成形特征

Fig. 1 Laser weld appearance of BT20 titanium alby

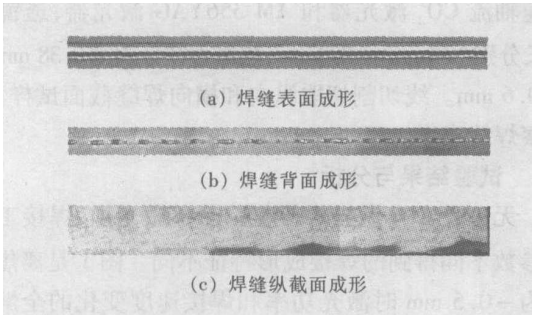


图 2 全熔透焊缝成形不稳定的焊缝背面和纵截面成形

Fig. 2 Back surface and longitudinal section of unstable full penetration weld

## 2 激光焊过程小孔形成机制

稳定熔透焊依赖于焊接过程穿透性小孔形成的稳定性。关于激光焊小孔形成机制, 多数学者认为是蒸气压力作用下激光与材料反应区的液体金属被去除的液体流动[4~8]。激光作用下, 金属表面吸收激光能量引起温度升高、熔化和气化, 熔化表面温度越高, 蒸气压力越大, 熔化表面受蒸气压力作用下凹形成小孔, 激光继续作用, 蒸气压力逐层将激光作用区的液体金属沿孔壁排挤开, 固 –液界面向金属内部推进, 金属如此被逐层熔化剥离, 最终形成一定深度的小孔。

连续激光焊时, 小孔相对于焊接方向是不对称的, 激光能量主要被小孔前壁吸收, 小孔形成的穿孔速度也取决于前壁产生的金属蒸气压力, 而蒸气压力的大小与液体金属层表面温度有关, 这涉及到小孔壁的能量平衡。Mastunawa等发现, 熔池中蒸气压力明显大于表面张力和液体静压力之和, 小孔前壁熔池金属高速流动。因此小孔前壁吸收的激光能量主要与气化损耗、金属中热传导和液体金属迁移传递的能量相平衡。

## 3 钛合金激光焊全熔透稳定条件计算

基于上述小孔前壁的能量平衡, 激光焊过程小孔的形成过程可简化见图 3. 激光作用区熔化金属在蒸气压力作用下沿孔壁迁移, 同时不断有新的固相金属熔化补充到。在稳定条件下, 固液界面和气液界面以同样的速度沿板厚方向推进, 厚度不变, 直

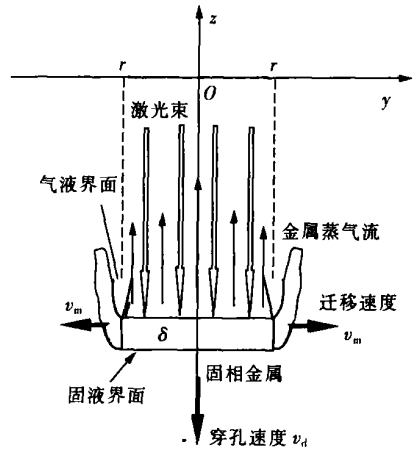


图 3 激光焊过程小孔形成物理模型示意图

Fig. 3 Sketch of keyhole formation during laser welding

至形成一定深度的小孔。Semak[6]曾根据能量平衡计算深熔焊穿孔速度,即设固相熔化速度与熔化金属迁移速度和气化速度相平衡,则固液界面移动速度即为穿孔速度。作者在此基础上确定稳定全熔透焊稳定条件。

相对于焊接方向将连续激光焊的激光作用区视为宽度为光斑直径矩形,激光作用区能量分布均匀,则单位时间内固态金属熔化量等于液体金属层迁移量与气化量之和,可表示为

$$2r\rho_s v_d = 2\delta\rho_m v_m + 2r\rho_m v_v, \tag{1}$$

式中:$r$为激光作用点的光斑半径;$\rho_s$,$\rho_m$为材料固态和液态密度;$v_d$,$v_m$和$v_v$分别为穿孔速度、液体金属层的迁移速度、金属的气化速度;$\delta$为激光作用区液体金属层的厚度,近似为$\delta \approx a_m / v_d$。则

$$v_d = \frac{1}{2}\left\{\frac{\rho_m}{\rho_s}v_v + \left[\left(\frac{\rho_m}{\rho_s}v_v\right)^2 + 4\frac{\rho_m a_m}{\rho_s r}v_m\right]^{\frac{1}{2}}\right\}。 \tag{2}$$

令$v_{dm}$和$v_{dv}$分别表示与液体金属层迁移和金属气化相关的穿孔速度分量,则由式(2)知,

$$v_{dm} = \frac{\rho_m}{\rho_s}\frac{\delta}{\delta}v_m,\quad v_{dv} = \frac{\rho_m}{\rho_s}v_v。$$

液体金属层迁移速度$v_m$与蒸气压力$p_r$相关,金属的气化速度$v_v$与表面温度$T_s$相关,其表达式分别为

$$v_m = \sqrt{\frac{2p_r}{\rho_m}}, \tag{3}$$

$$v_v = v_c \exp\left(-\frac{m_a L_v}{N_a K_b T_s}\right), \tag{4}$$

$$p_r = AB_0 (T_s)^{-\frac{1}{2}} \exp\left(-\frac{m_a L_v}{N_a K_b T_s}\right)。 \tag{5}$$

式中:$A$为常数,取决于室温压力;$B_0$为蒸气常数;$m_a$为原子质量;$N_a$为阿加德罗常数;$K_b$为波尔兹曼常数;$L_v$为金属的气化潜热;$T_s$为液体金属层表面温度;$c$为蒸气中的声速。

稳态时小孔壁沿焊接方向单位长度上获得的能量$P_{in}$为液体层直接吸收的激光能量与固相金属熔化所需能量之和,部分被金属蒸气带走($P_1$),液体层吸收的能量部分通过热传导($P_2$)和对流($P_3$)向四周传递,根据能量平衡各表达式为

$$P_{in} = 2I_a r + 2\rho_s c_s T_m v_d r; \tag{6}$$

$$P_1 = 2\rho_m v_v L_v r; \tag{7}$$

$$P_2 = 2\rho_s c_s (T_m - T_0) v_d r + 2r\frac{\rho_s c_s (T_m - T_0) v_d}{l}, \tag{8}$$

$$P_3 = 2\rho_m (c_m T_a + L_m) v_m \delta \approx 2\rho_m (c_m T_a + L_m) v_m \frac{a_m}{v_d}, \tag{9}$$

式中:$I_a$为激光作用于液体层表面的功率密度;$c_s$为固态金属比热容;$T_m$为金属熔点;$T_0$为固相金属初始温度;$T_a$为液体金属层平均温度,取$T_a = T_m + 0.5(T_s + T_m)$;$a_m$,$a_s$为液相和固相金属的热扩散系数;$l$为由液体金属层侧面热传导的等效长度。可由式(10)计算

$$l = \left[\frac{a_s}{v_d}\left(r + \frac{a_m}{v_d}\right)\right]^{1/2} = \left(\frac{a_m}{a_s} + \frac{v_d}{a_s}r\right)^{1/2}。 \tag{10}$$

由式(6)~式(10)得激光焊过程维持小孔稳态形成时小孔壁面所需的最小激光功率密度为

$$I_a = \left(\rho_m (c_m T_a + L_m)\frac{v_m a_m}{v_d r} - \rho_s c_s T_0 v_d\right) + \frac{\rho_s c_s (T_m - T_0) v_d}{\left(\frac{a_m}{a_s} + \frac{v_d}{a_s}r\right)^{\frac{1}{2}}} + \rho_m v_d L_v。 \tag{11}$$

将钛合金的热物理性能和激光焦斑半径带入以上公式,即得穿孔速度和金属熔化速度与穿孔所需的激光功率密度之间的关系。图 4为钛合金 $CO_2$ 激光焊穿孔速度与激光作用区功率密度之间的关系。从图 4可看出,穿孔速度与激光功率密度成正比,液体金属的迁移在小孔的形成过程起主要作用。在所研究条件下,钛合金两种激光焊的穿孔速度与激光功率密度的函数线性关系为

$$v_{dCO_2} = 0.23 I_a - 0.009,\tag{12}$$

$$v_{dYAG} = 0.24 I_a - 0.013。\tag{13}$$

式(12)、(13)可计算钛合金激光焊所选焊接工艺参数下的穿孔速度。因熔透焊的穿孔速度应与焊接速度匹配,设光斑以焊接速度$v$移动一个光斑直

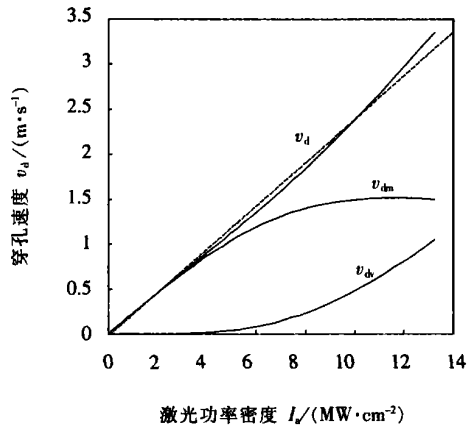


图 4　激光穿孔速度与激光功率密度间的关系

Fig. 4　Relationship between drilling speed and laser power intensity

径需要时间 $t_w$，激光穿透板厚 $d$需要时间 $t_d$，若 $t_d < t_w$，可保证全熔透焊接，$t_d = t_w$ 对应的激光功率密度就是临界全熔透焊所需最小激光功率密度。表 1为 2 5mm厚板钛合金实际焊接过程的激光功率密度 $I_0$ 与穿孔所需激光功率密度 $I_a$ 计算结果的比较。可见，$CO_2$ 激光焊额计算值基本上是试验值的一半，而 YAG激光焊的计算值与试验值接近，这反映了钛合金 $CO_2$ 激光焊受等离子体的影响比 YAG激光焊大，激光功率密度损耗也较大，与一些研究认为 $CO_2$ 激光焊功率损耗可达一半的结果是一致的。

表 1 全熔透焊所需最小激光功率密度计算值与试验实际值

Table 1 Calculation and experimental result of threshold of laser power density for full penetration

| 焊接方法 | 焊接速度 $v$/(m·min$^{-1}$) | $t_d$/s | $t_w$/s | $I_a$/(MW·cm$^{-2}$) | $I_0$/(MW·cm$^{-2}$) |
|---|---|---|---|---|---|
| $CO_2$ 激光焊 | 1.5 | 0.0152 | 0.164 | 0.75 | 1.5 |
| | 3.0 | 0.0076 | 0.329 | 1.47 | 2.65 |
| YAG激光焊 | 1.5 | 0.024 | 0.104 | 0.52 | 0.53 |
| | 3.0 | 0.012 | 0.208 | 0.93 | 1.06 |

## 4 结 论

由于金属蒸气和光致等离子体的作用，钛合金激光深熔焊过程存在全熔透不稳定现象，其特征是焊缝表面均匀，焊缝背面交替出现熔透与未熔透，其不稳定过程与穿孔稳定性密切相关，为此根据激光焊孔壁能量平衡，提出了小孔穿孔速度与焊接速度相匹配的熔透稳定性物理模型，可针对材料和板厚确定激光全熔透焊所需最小激光功率密度，建立穿孔速度与焊接速度、最小激光功率密度之间的关系，对焊接工艺参数的熔透稳定性进行判断。

参考文献：


[1] 王家淳. HE130钛合金激光焊接工艺及接头组织性能研究[D]. 北京：北京有色金属研究总院，2001.

[2] 陈武柱，张旭东，等. 激光焊接时焊接模式转变规律及焊接过程稳定性的研究[J]. 中国激光，1996，23(7)：657－661.

[3] Miyamoto I, Maruo H, Arata Y. The role of assistant gas in $CO_2$ laser welding[J]. ICALEO, 1992: 68－74.

[4] Semak V, Mastunawa A. The role of recoil pressure in energy balance during laser materials processing[J]. Journal of Physics D: Applied Physics, 1997, 30: 2541－2552.

[5] Trappe J, Kroos J, Tix C, *et al*. On the shape and location of the keyhole in deep penetration laser welding[J]. Journal of Physics D: Applied Physics, 1994, 27: 2152－2254.

[6] Semak V, Hopkins JA, McCay M H, *et al*. Melt pool dynamics during laser welding[J]. Journal of Physics D: Applied Physics, 1995, 28: 2443－2450.

[7] Mastunawa A, Semak V. The simulation of the front keyhole wall dynamics during laser welding[J]. Journal of Physics D: Applied Physics, 1997, 30: 798－809.

[8] Kaplan A. A model of deep penetration laser welding based on calculation of the keyhole profile[J]. Journal of Physics D: Applied Physics, 1994, 27: 1805－1814.


作者简介：陈 俐，女，1966年 5月出生，博士研究生，高级工程师。研究方向为材料激光加工和焊接性，发表论文 20余篇。

Email: ouchenxi@163.com

icular ferrite fraction, but too much acicular ferrite microstructures leads to accelerate corrosion of weld in HSLA.

**Key words**: high strength low alloy steel; SAW; acicular ferrite; corrosion; polarization resistance

**Mathematical model of the stable full penetration laser welding for titanium alloy sheet** CHEN Li[1,2], HU Lun-ji[1], GONG Shui-li[2] (1. Huazhong University of Science and technology, Wuhan 430074, China; 2. Key Lab for High density beam manufacture technology, Beijing aeronautic manufacturing technology research institute, Beijing 100024, China). p35 - 38

**Abstract**: The macrostructure of laser welding for titanium alloy was investigated in this paper. The results show that unstable full penetration will occur because of influence of laser induced plasma, even though laser welding parameters were stable. This phenomenon was characterized by perfect weld surface, and unstable weld back that part penetration and full penetration formed by turns. It is assumed that unstable full penetration was intrinsic for laser penetration welding and depended on significantly the drilling speed during the keyhole forming. According to the energy balance on keyhole wall, the mathematical model for the smallest laser power density that made the stable full penetration weld was suggested in this paper, which allowed laser power density to be related to material properties, sheet thickness the, drill speed and laser welding speed. The computed results were corresponded with the experimental results.

**Key words**: titanium alloy; laser welding; full penetration; welding stability calculation

**Influnce of process parameters on appearance of plasma-melt-sprayed WC-17%Co coatings** ZHAO Min-hai, LIU Ai-guo, GUO Mian-huan, LIU De-Jian, (National Key Laboratory of Advanced Welding Production Technology, Harbin Institute of Technology, Harbin 150001, China). p39 - 42

**Abstract**: Ceramic coatings can be metallurically bonded to metal sabstrate with plasma-melt-spraging, which has virtue of both plasma spray and harfacing. Coralt-based WC is hard, wear-reristant, corrosion-resistant and thermal-resistant. WC-17% Co coating was plasma-melt-sprayed on Q235 substrate. Influnce of proceis parameters (angle between plasma melting torch and spraying torch, distance between the plasma torch and the substrate, velocity of melting and spraying and feeding rate of powder) on appearamce of the coating was investigated, and the pavameters were optimized. Metallurgically bonded coating without defects was obtained.

**Key words**: plasma melt spraying; WC-17% Co coating, parameter, appearame

**Microstructures and properties of TC4 alloy joints welded by the electron beam welding** XU Hong-ji[1], YIN Li-xiang[1], LI Jin-wei[2], XIE Ming[1] (1. School of Materials Science and Engineering, Dalian Jiaotong University, Dalian 116028, China; 2. Beijing Aeronautical Manufacturing Technology Research Institute, Beijing 100024, China). p43 - 46

**Abstract**: Microstructures and properties of TC4 alloy joints welded by electron beam welding were investigated with room-temperature tensile test, room-temperature notch tension test, microhardness test and metallographic analysis. The results showed that the joints with good performance of TC4 alloy may be obtained by means of electron beam welding (EBW). The tensile strength of welded joint is not less than that of the base metal, and the notch sensitive coefficient of the welded joint is less than 1. The hardness of the welded joint and the HAZ are higher than that of the base metal. The microstructure of the weld metal is $\alpha'$ phase (needle martensite) which was transformed from the primary coarse $\beta$ matrix, and that of the HAZ was the mixture of fine needle martensite and the primary $\alpha$ phase.

**Key words**: TC4 alloy; electron beam welding; welded joint

**Study on heat transfer of melt pool in laser keyhole welding** WANG Hong[1,2], SHI Yao-wu[1], GONG Shui-li[2], (1. School of Materials Science and Engineering Beijing university of Technology, Beijing 100022, China; 2. Beijing aeronautical manufacture technology research institute, Beijing 100024, China). p47 - 50

**Abstract**: The shape of welding pool in laser deep penetration welding was calculated based on continuity equation, momentum conservation equation and energy conservation equation using FLUENT solver. Solidification/Melting model and $\kappa - \varepsilon$ model were used. Simulation results showed that the recoil pressure on the front wall of the keyhole is an important driving force of welding pool fluid flow because of large temperature gradient in the front part. The larger size of the solidification transition zone of welding pool in the liquid-solid interface was related to solidification heat.

**Key words**: laser welding; simulation; molten pool; titanium alloy